6-2021

Simplified structural analysis of framed ordinary non-tempered glass panels during fire exposure

Amer Sabsabi
The University of Western Ontario

Maged A. Youssef
Western University, youssef@uwo.ca

Salah El-Din F. El-Fitiany
The University of Western Ontario

Ajitanshu Vedrtnam
Invertis University

Citation of this paper:
Sabsabi A., **Youssef M.A.**, El-Fitiany SF, Vedrtnam A, 2021, "Simplified structural analysis of framed ordinary non-tempered glass panels during fire exposure", Fire Safety Journal, 122: 103357, https://doi.org/10.1016/j.firesaf.2021.103357

Simplified Structural Analysis of Framed Ordinary Non-Tempered Glass Panels during Fire Exposure

A. Sabsabi [1], M.A. Youssef [1,*], S.F. El-Fitiany [1,2], A. Vedrtnam [3]

[1] *Western University, Department of Civil and Environmental Engineering, London, ON, N6A 5B9 Canada.*
[2] *Alexandria University, Department of Structural Engineering, Alexandria, Egypt*
[3] *Invertis University, Department of Mechanical Engineering, Bareilly, UP, India-243001*

Abstract

Ordinary non-tempered glass is one of the most widely used materials in the construction industry. Knowing its fire resistance is essential to ensure the safety of emergency personnel as its failure increases the oxygen supply and causes a rapid spread of the fire (flashover phenomenon). Existing approaches for evaluating the structural fire safety of glass façades require expensive experimental tests and/or extensive knowledge of Finite Element modeling. This paper provides a simplified, rational, and reliable approach to assess the structural capacity of ordinary glass panels during fire exposure. A simplified method is developed to predict the temperature difference between the edge and the center of the glass panel. Afterwards, a method, based on strain-equilibrium, is developed to predict the corresponding maximum thermal stress. The developed methods are validated by comparisons with experimental work by others.

Keywords: Façade; glass; fire exposure; thermal exposure; Finite Element, numerical modelling

* Corresponding Author. Tel.: +1 519 661 2111, 88661; E-mail address: youssef@uwo.ca (Youssef, M.A.).

1. Introduction

Fire safety has been mostly restricted to structural elements. Consequently, the interaction between the non-structural elements, e.g. glazing and façade elements, and the fire has been overlooked [1]. Nevertheless, recent tragic incidents (e.g., Grenfell Tower fire, UK) emphasized the key role of non-structural elements during fire incidents [2].

During a fire incident, failure of glass panels creates new vents, which increases the oxygen supply, leading to a wide spread of smoke and flames. This failure is caused by the thermal gradient between the center and edge of the glass panels [3–5]. These thermal gradients occur because of the thermal isolation provided by the supporting frame and the glass low thermal conductivity. Ordinary glass or float glass is the basic product of the floating process and is mainly composed of silica with other added oxides to improve its chemical and physical properties. It is usually non-tempered, which mean it has minimal residual stresses at its surface.

Several experimental [6–15] and numerical studies [16–19] were conducted to predict the thermal and structural behavior of glass panels during fire incidents. These studies highlighted the key factors, which affect the fire resistance of glass panels, including the applied heat flux [7,20], fire location [8,9], temperature gradients [14], size of glass panels [12,18,19], edge finishing conditions [16], and installation method [13,21]. The finite element models [16–19] relied on the experimentally measured temperatures to define the boundary conditions. To estimate the glass temperature numerically, Pagni and Joshi [4] proposed a dimensionless equation that can be used to predict the temperature field in glass panels during fire exposure. However, the equation is mathematically complex to solve as it requires computing three kernels and a complementary error function. Harada et al. [7] proposed an equation to calculate the thermal breakage stress for glass panels during fire exposure as a function of the

temperature difference between the center and edge of the glass panel. However, the breakage stress was assumed to be independent of the glass panel dimensions.

Much of the current literature about fire safety of glass relies on experiments or advanced analysis using finite element method. These approaches are expensive and/or time-consuming. To the best of the authors' knowledge, the literature is lacking simplified analysis techniques that can facilitate applying performance-based design concepts, while designing building facades. This paper addresses this research gap by providing a simple approach to accurately predict the thermal stresses in framed ordinary non-tempered glass panels during fire exposure. The approach provides the means to predict the temperature gradient caused by fire exposure and then, predict the maximum developed thermal stress.

2. Temperature of Glass during Fire Exposure

In this section, a simplified approach is developed to predict the temperatures at the center and at the edge of glass panels exposed to fire. The part of the glass panel, which is covered by the supporting frame, is assumed to be unaffected by radiation and convection of the flames. Therefore, it is only heated through conduction from the exposed part of the glass. This assumption simplifies the complex heat transfer system, shown in Fig. 1a, and eliminates the need for considering the heat exchange between the frame and glass leading to a simple heat transfer system, which is shown in Fig. 1b. This assumption will result in a higher estimate for the temperature difference in the glass panel, which will lead to a conservative estimate for its fire endurance. The approach starts by deriving a heat transfer equation to determine the temperature at the center of the glass panel, and then, uses this temperature to evaluate the temperature of the protected part.

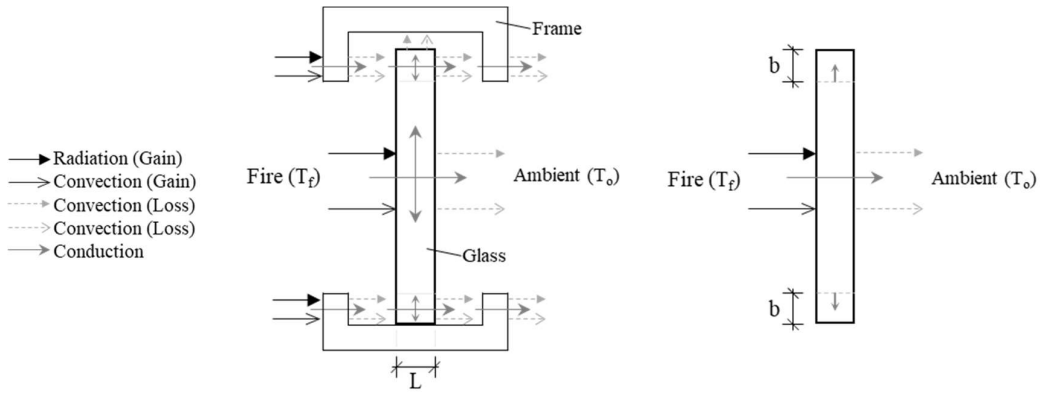

(a) Actual (b) Proposed simplification

Fig. 1. Heat transfer system for glass during fire exposure

2.1 Temperature at the center of the glass panel

During an actual fire, temperature of the glass panel depends on many factors including the location of the fire relative to the panel, size of the panel, and air movement within the compartment. In this paper, it is assumed that the uncovered glass surface is exposed to a uniform fire temperature. This assumption has been previously used in the literature [18–24]. Furthermore, the temperature gradient across the glass panel thickness is assumed to be uniform. This assumption is based on the fact that the Biot number ($Bi = \frac{hL_c}{\lambda}$) of typical glass panels is expected to be less than or equal 0.1, where L_c can be taken equal to the glass thickness (L). such a value for *Bi* means that the resistance to conduction within the glass is much less than the resistance to convection at the air boundary layer [25].

Given the above-mentioned assumptions and knowing that energy generated within the glass is zero, the conservation of energy at any time instant *t* for the system shown in Fig. 1b can be expressed by Eq. 1,

$$\dot{E}_{in} - \dot{E}_{out} = \frac{dE_{st}}{dt} \quad (1)$$

Where $\dot{E}_{in}$ and $\dot{E}_{out}$ are the rates of energy transferred into and out of the glass panel, respectively, and E_{st} is the rate of energy stored in the system. As the energy transfer is happening due to convection and radiation, Eq. 1 can be rewritten in the following form,

$$q_{gain,con} + q_{gain,rad} - q_{loss,con} - q_{loss,rad} = \rho c \frac{dT}{dt} \quad (2)$$

Where $q_{gain,con}$ and $q_{gain,rad}$ are the rates of heat gain from convection and radiation, respectively, and $q_{loss,con}$ and $q_{loss,rad}$ are the rates of heat loss from convection and radiation, respectively. ρ and c are the glass' density and specific heat, respectively. Substituting with the convection and radiation heat rate equations, Eq. 2 can be written as,

$$\Delta T = \frac{\Delta t}{\rho c L}\left[h_f\left(T_\infty - T_g\right) + \varepsilon\sigma\left({T_\infty}^4 - T_g^4\right) - h_b\left(T_g - T_i\right) - \varepsilon\sigma\left(T_g^4 - {T_i}^4\right)\right] \quad (3)$$

Where Δt is the time increment, ε is the emissivity of the glass and can be assumed equal to 0.85 [22], σ is the Stefan–Boltzmann constant, and h_f and h_b are the film coefficients at the fire and ambient sides, respectively. Eq. 3 can be utilized to calculate the temperature of the glass at each time step for both standard and natural fire curves using a simplified spreadsheet.

The values of h_f and h_b can be computed utilizing existing empirical equations by Incropera et al. [25]. For the case of vertical glass panel, the value of h can be calculated using the following empirical equation,

$$h = \frac{0.59 \cdot k \cdot (G_r P_r)^{\frac{1}{4}}}{l} \quad (4)$$

Where, l is the flame height and can be taken equal to the window height, k is the thermal conductivity of air, G_r is Grashof number, P_r is Prandtl number, and G_r and P_r can be computed from the following equations,

$$G_r = \frac{g \cdot l^3 \cdot \beta \cdot (T_\infty - T_g)}{{\nu_a}^2} \quad (5)$$

$$P_r = \frac{\nu_a}{\alpha} \quad (6)$$

$$\beta = \frac{1}{T_\mathrm{f}} \quad (7)$$

Where, T_∞ is the temperature of the air, T_g is the temperature of the glass surface, g is the gravitational acceleration, ν_a is the kinematic viscosity of the air, α is the thermal diffusivity of the air, β is the thermal expansion coefficient of the air, and T_f is the film temperature and can be calculated as the average temperature between the air and the glass surface [26]. The air temperature is taken equal to the fire temperature at the exposed side of the glass and the ambient temperature (T_i) at the unexposed side of the glass. Eq. 4 can be used based on a conservative and widely used assumption in structural fire engineering, which assumes the fire and air are stagnant inside the fire compartment. This assumption leads to free convection between the air and the glass panel. For this case, the convection heat transfer coefficient, film coefficient (h), typically ranges from 5 to 25 W/m^{2}K [27].

2.2 Temperature at the edge of the glass panel

Based on the assumption that the edge of the glass panel is only heated via conduction from the exposed parts, a parametric study was necessary to determine the ratio between the temperature of the protected part (T_e) and the temperature of the exposed part (T_g). The commercial software ABAQUS [28] was utilized for that purpose. Heating of the exposed part of the glass, Fig. 2a, was simulated as uniform surface interaction that involved radiation and convection. For such a case, the change in the glass dimensions do not affect the ratio between T_e and T_g. The only parameters that need to be considered are the glass thickness (L), width of the frame (b), and the fire scenario. Fifteen Glass thicknesses covering range from 1 to 15 mm

and ten widths for the supporting frame covering range from 5 to 50 mm were considered in the analysis. These ranges deemed to cover most of the practical values available in the literature. Assuming ISO 834 temperature-time relationship [29], 150 cases were analyzed. It should be noted that the analysis cases also represent the heating region of natural fire curves.

The material properties were assumed as follows ρ = 2500 kg/m^3 and c = 820 J/kg·K. The glass was initially assumed to be at the ambient temperature, T_i of 20°C, and heat losses were assumed to only occur at the ambient side. The glass panel was modeled using 8-node-3D linear-heat transfer brick elements (DC3D8 type from ABAQUS library). A maximum mesh size of 10 mm was utilized, as it was found to result in acceptable accuracy. Using a smaller mesh size did not affect the accuracy of the results, and significantly increased the computational time. For example, reducing the mesh size from 10 mm to 5 mm did not change the value of T_g and resulted in T_e difference of less than 5%, but it increased the computation time by 180%. An example of the generated mesh is shown in Fig. 2b. The average temperature at point A, which is at the middle of the glass panel edge, as shown in Fig. 2a, was recorded for each run. A typical temperature distribution, as produced by ABAQUS, is shown in Fig. 3. Also, the typical variation of the ratio $\frac{T_e}{T_g}$ with time is shown in Fig. 4.

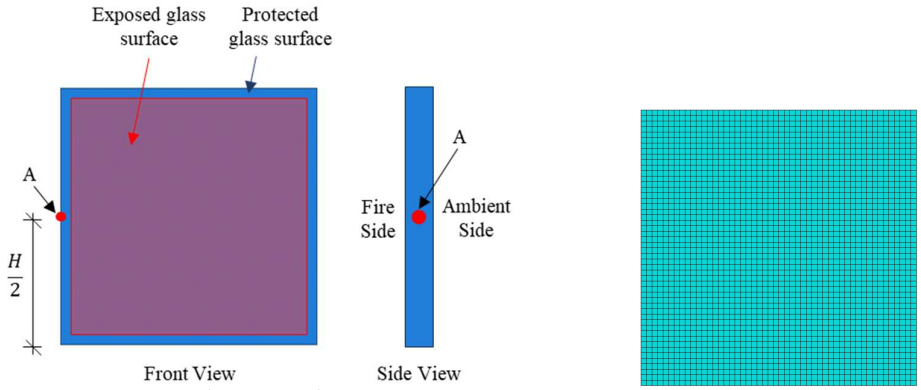

(a) glass panel zones (b) generated mesh

Fig. 2. Glass Panel Simulation using ABAQUS

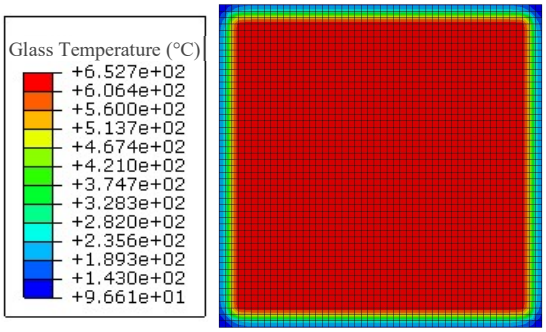

Fig. 3. ABAQUS Temperature Distribution (L = 6 mm, b = 20 mm, t = 30 minutes)

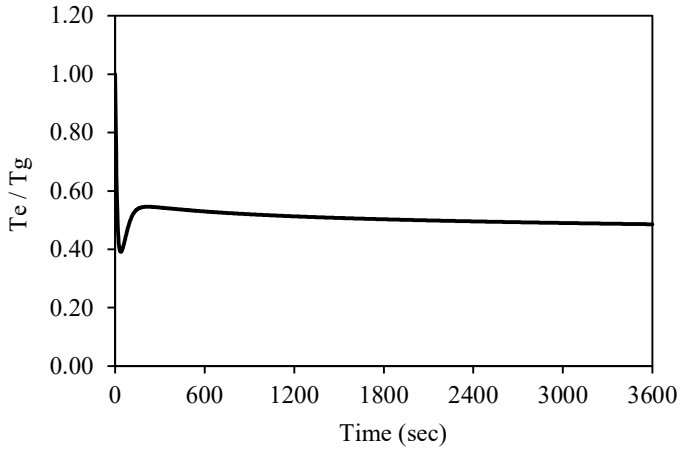

Fig. 4. Variation of $\frac{T_e}{T_g}$ with time (L = 1 mm and b = 5 mm)

Initially, the exposed and protected parts of the glass had the same temperature, and, then the ratio between their temperatures started to change until reaching a constant value. Considering all examined cases, the average $\frac{T_e}{T_g}$, for the relatively constant part of the variation, is given in Fig. 5 as function of the frame width and glass thickness. The temperature difference between the center and edge of the glass panel increases with increasing the glass thickness and decreases with increasing the frame width. Engineers can utilize this figure to calculate this ratio, which can be used calculate the temperature of the glass edge in terms of the temperature at the glass center. To further simplify calculation of $\frac{T_e}{T_g}$, the figure data were utilized to develop

the formula given by Eq. 8, which allow calculating $\frac{T_e}{T_g}$ as function of b (m) and L (m). The equation and coefficients were determined using a least square regression analysis, common regression requirements of probability (p) < 0.0001 and correlation (R^2_{adj}) > 95% were maintained. The maximum error associated with using Eq. 8 is less than 6%, as shown in Fig. 6.

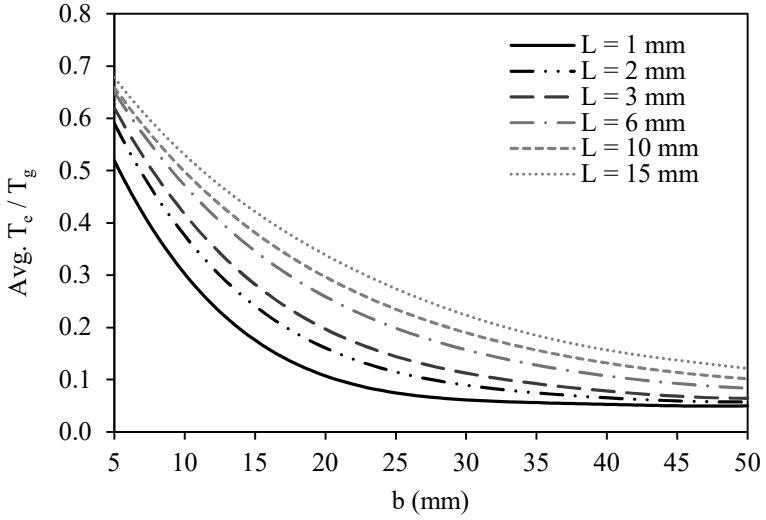

Fig. 5. Evaluation of $\frac{T_e}{T_g}$ as function of b and L

$$\begin{aligned}\frac{T_e}{T_g} = {} & + 0.739 \times 10^0 \times 1 - 81.44 \times 10^0 \times b \\ & + 134.7 \times 10^0 \times L + 833.5 \times 10^0 \times b{\times}L \\ & + 3.345 \times 10^3 \times b^2 - 31.25 \times 10^3 \times L^2 \\ & - 201.6 \times 10^3 \times b^2{\times}L + 606.4 \times 10^3 \times b{\times}L^2 \\ & - 62.69 \times 10^3 \times b^3 + 3.160 \times 10^6 \times L^3 \\ & + 2.300 \times 10^6 \times b^2{\times}L^2 + 3.550 \times 10^6 \times b^3{\times}L \\ & - 52.00 \times 10^6 \times b{\times}L^3 + 536.0 \times 10^3 \times b^4 \\ & - 155.0 \times 10^6 \times L^4 - 55.40 \times 10^6 \times b^3{\times}L^2 \\ & + 101.0 \times 10^6 \times b^2{\times}L^3 - 17.60 \times 10^6 \times b^4{\times}L \\ & + 1.280 \times 10^9 \times b{\times}L^4 - 1.590 \times 10^6 \times b^5 \\ & + 3.040 \times 10^9 \times L^5 \end{aligned} \quad (8)$$

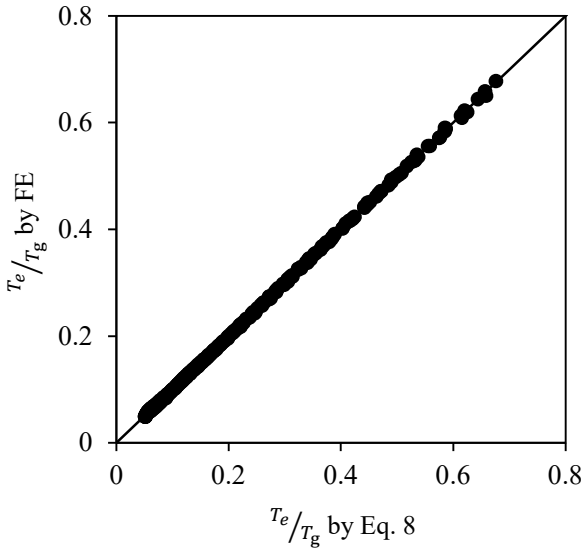

Fig. 6. Accuracy of using Eq. 8 in predicting $\frac{T_e}{T_g}$

2.3 Validation

The experimental test conducted by Chen et al. [23] was utilized to validate the proposed heat transfer method. Test 1 by Chen et al. [25] involved heating a 600 mm by 600 mm by 6 mm ordinary glass panel using a natural fire curve. The width of the protected part was 10 mm. Eq. 3 was first used to predict the temperature at the glass center. Afterward, $\frac{T_e}{T_g}$ was evaluated using Eq. 8 and found to be equal to 0.474. As shown in Fig. 7a, the results of the proposed approach are in good agreement with the experimental study. It should be noted that Eq. 8 is only valid after the ratio $\frac{T_e}{T_g}$ becomes constant, which is at about 250 second for this sample. However, the use of a constant ambient temperature for the duration before the 250 second seems to provide good results.

To further validate the proposed method, the experimental tests conducted by Harada et al. [7] and Zhao et al. [30] were considered. The glass panel dimensions were 500 mm by 500 mm by 3 mm and 600 mm by 600 mm by 6 mm, respectively. The width of the covered part was 15 mm and 10 mm, respectively. Figs. 7b and 7c show that the proposed approach predicted

the temperature at the center and edge of the glass panels with good accuracy. The small differences between the experimental and numerical results can be due to experimental errors, or numerical assumptions including: (1) uniform temperature across the glass thickness, (2) constant glass thermal properties, and (3) ignoring radiation and convection for the covered part of the glass panel.

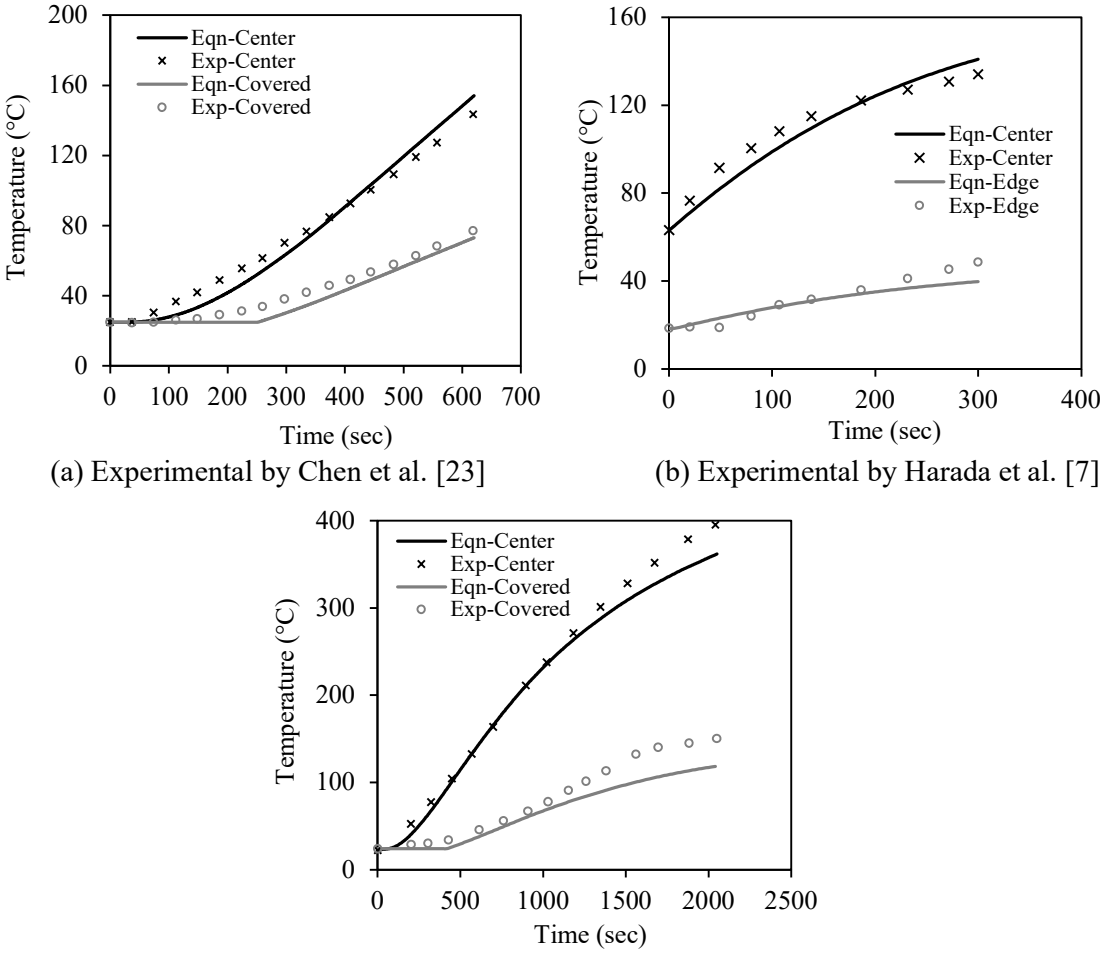

(a) Experimental by Chen et al. [23]

(b) Experimental by Harada et al. [7]

(c) Experimental by Zhao et al. [30]

Fig. 7. Validation of the Proposed Approach

3. Maximum Developed Thermal Stress

The second step in the proposed approach is to determine the maximum developed thermal stress. The following subsections provide the development of a simplified method to estimate the maximum thermal stress, and then generalize the simplified method to be applicable for any temperature distribution.

3.1 Proposed simplified method

Fig. 8a shows a glass panel, with dimensions W by H, and a frame width b. The connection between the panel and the frame was assumed to have enough clearance to allow for free expansion [3,10,18]. During fire exposure, the temperature in the protected part is much lower than the temperature of the exposed part. The resulting unrestrained thermal strain distribution (ε_{th}) is shown in Fig. 8b. This free-thermal expansion cannot develop, as the glass is expected to follow the plane section assumption. Thus, a self-induced strain (ε_s), Fig. 8c, is expected to develop to convert the free thermal strain to an equivalent linear strain ($\overline{\varepsilon_{th}}$), which is uniform for the presented case because of the symmetry of the unrestrained thermal strains. The uniform strain, ε_i, shown in Fig. 8d reflects the actual deformation of the glass. This concept was previously adopted by El-Fitiany and Youssef [31], while analyzing reinforced concrete cross sections exposed to fire.

The self-induced strains must be in-self equilibrium. They can be divided into internal compressive strains (ε_{sc}) for the exposed glass area and tensile strains (ε_{st}) for the protected glass area (Fig. 8c). These tensile strains correspond to the maximum tensile stresses, which will develop in the glass sample.

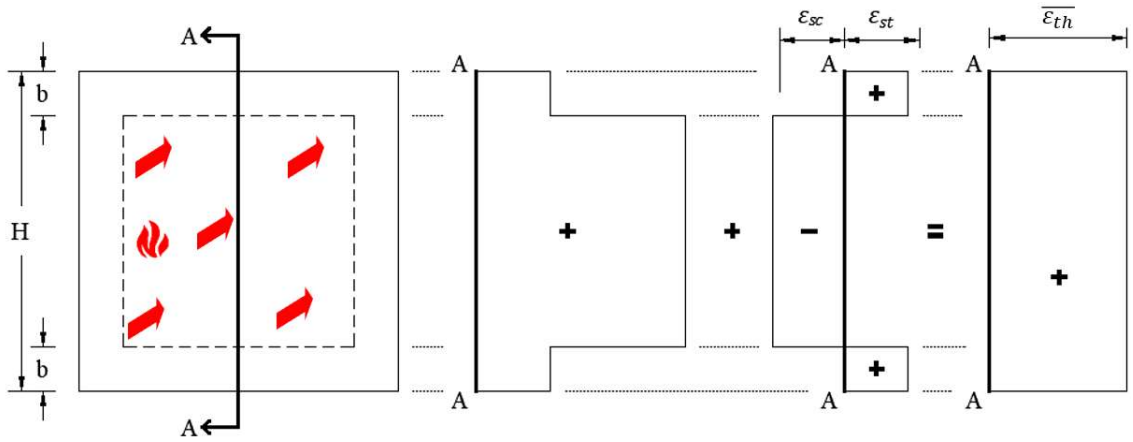

(a) Heated glass panel (b) ε_{th} (c) ε_s (d) $\overline{\varepsilon_{th}}$

Fig. 8. Developed strains in uniformly heated glass panel

Eq. 9 can be derived based on the uniform total strain, and from the equilibrium of the self-induced forces, Eq. 10 can be written.

$$\varepsilon_{st} + \alpha_g \times T_e = \alpha_g \times T_g - \varepsilon_{sc} \quad (9)$$

$$\varepsilon_{sc} \times E \times (\mathrm{H} - 2\mathrm{b}) \times \mathrm{L} = \varepsilon_{st} \times E \times 2\mathrm{b} \times \mathrm{L} \quad (10a)$$

$$\varepsilon_{st} = \varepsilon_{sc}\left(\frac{\mathrm{H}}{2\mathrm{b}} - 1\right) \quad (10b)$$

Where α_g and E are the glass' thermal expansion coefficient and modulus of elasticity, respectively. The value of the self-induced tensile thermal strain can then be obtained by solving equations 9 and 10b, which results in Eq. 11.

$$\varepsilon_{st} = \alpha_g\left(T_g - T_e\right)\left(1 - \frac{2\mathrm{b}}{\mathrm{H}}\right) \quad (11)$$

Eq. 11 indicates that the self-induced tensile strain increases with the increase of the height of the glass panel (H) and the difference in temperature between the exposed and protected regions. It decreases with the increase of width of the protected area (b). These findings are in agreements with the findings of previous experiments [11,18,32]. It should be noted that the

factor $\left(1-\frac{2b}{H}\right)$ is consistent with the geometric factor proposed by Pagni and Joshi [4,10] and Pagni [10], which was developed based on a hyperbolic temperature variation. Using the previously evaluated temperatures at the center and edge of the glass panel, engineers can utilize equation 11 to estimate the maximum internal thermal stress in the glass panel.

3.2 Generalization of the proposed simplified method

In a real fire scenario, the glass panel is expected to have a variable temperature profile. This section explores the use of the developed simplified method for the case of linearly varying temperature profile. The derivation, shown below, can be modified to accommodate other temperature distributions.

Fig. 9a shows a glass panel, exposed to higher average temperatures at its top than its bottom. The temperature within the width b was assumed to be constant with values T_{et} at the top and T_{eb} at the bottom. The temperature of the exposed region of the glass panel was assumed to be varying linearly from T_{gt} at the top to T_{gb} at the bottom. This linear temperature distribution is a simplification for real situations where the temperature of the upper layers of air is higher than the lower ones (stack effect) due the convection of compartment fires. The resulting unrestrained thermal strains (ε_{th}), Fig. 9b, are ε_{th-et} at the top covered region, ε_{th-eb} at the bottom covered region, ε_{th-gt} at the top of the exposed region, and ε_{th-gb} at the bottom of the exposed region. Self-induced strains (ε_s), Fig. 9c, are expected to be developed to maintain the linearity of the thermal profile. The equivalent linear strain profile ($\overline{\varepsilon_{th}}$) is expected to be variable in this case with a middle strain ε_i and a curvature ψ_i.

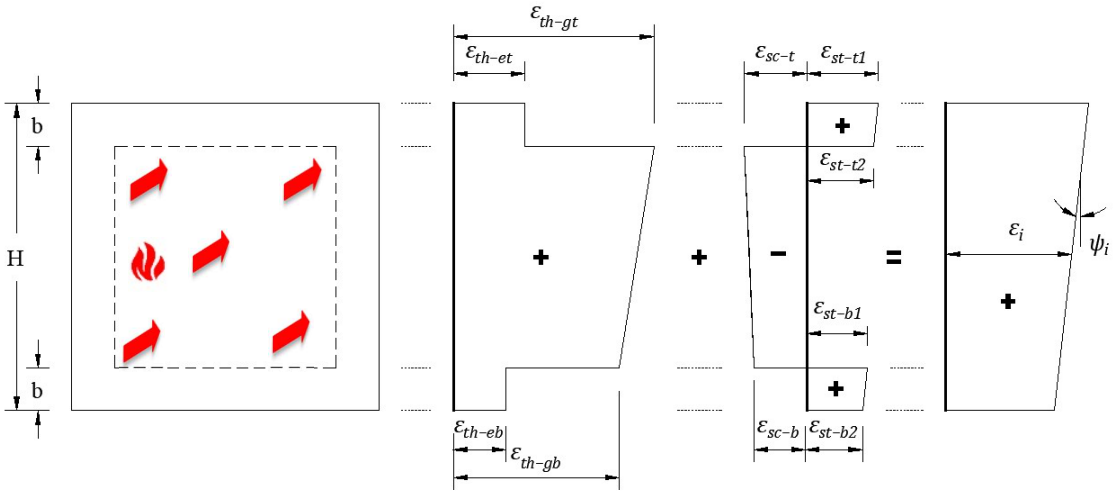

(a) Heated glass panel (b) ε_{th} (c) ε_s (d) $\overline{\varepsilon_{th}}$

Fig. 9. Developed strains in a glass panel heated at its top more than its bottom

The self-induced thermal strains can be expressed in terms of the equivalent thermal strains and the unrestrained thermal strains using the following equations.

$$\varepsilon_{st-t1} = \varepsilon_i + \psi_i \frac{\mathrm{H}}{2} - \varepsilon_{th-et} \tag{12a}$$

$$\varepsilon_{st-t2} = \varepsilon_i + \psi_i \frac{\mathrm{H} - 2\mathrm{b}}{2} - \varepsilon_{th-et} \tag{12b}$$

$$\varepsilon_{st-b1} = \varepsilon_i - \psi_i \frac{\mathrm{H} - 2\mathrm{b}}{2} - \varepsilon_{th-eb} \tag{12c}$$

$$\varepsilon_{st-b2} = \varepsilon_i - \psi_i \frac{\mathrm{H}}{2} - \varepsilon_{th-eb} \tag{12d}$$

$$\varepsilon_{sc-t} = \varepsilon_i + \psi_i \frac{H - 2b}{2} - \varepsilon_{th-gt} \tag{12e}$$

$$\varepsilon_{sc-b} = \varepsilon_i - \psi_i \frac{\mathrm{H} - 2\mathrm{b}}{2} - \varepsilon_{th-gb} \tag{12f}$$

Where ε_{st-t1}, ε_{st-t2}, ε_{st-b1} and ε_{st-b2} are the self-induced tensile strains at the top and bottom edges of the covered areas as demonstrated in Fig. 9c. ε_{sc-t} and ε_{sc-b} are the self-induced compressive strains at the top and bottom of the exposed part of the glass.

Eqs. 13 and 14 can then be derived based on equilibrium of forces and moments resulting from the self-induced strains.

$$\varepsilon_i = \frac{\alpha_g \mathrm{b}}{\mathrm{H}}(T_{et} + T_{eb}) + \frac{\alpha_g(\mathrm{H} - 2\mathrm{b})}{2\mathrm{H}}\left(T_{gt} + T_{gb}\right) \tag{13}$$

$$\psi_i = \frac{\alpha_g(6bH - 6b^2)}{H^3}(T_{et} - T_{eb}) + \frac{\alpha_g(H - 2b)^2}{H^3}\left(T_{gt} - T_{gb}\right) \tag{14}$$

4. Validation

The proposed approach is used to calculate the tensile stress generated during fire exposure of different glass panels given in the literature. Table 1 provides a summary of the validation cases. Wang et al. [18] experimentally tested ordinary non-tempered glass panels (E = 67 GPa, ρ = 2500 kg/m^3, and α_g = 8.5 × 10^{-6} 1/°C) with dimensions of 300 mm by 300 mm by 6 mm, which were protected at the edges by a frame width of 20 mm. The glass panels were heated in a small air compartment using a heating panel. The heating rate was 10 ºC/min until the air reached a temperature of 600 ºC, which was kept constant for a period of 20 minutes. Wang et al. [18] had also developed a FE model to study the effect of the glass panel dimensions on its behavior during fire exposure. Dimensions ranging from 100 mm to 1000 mm and aspect ratios of 400:1, 100:1, 25:1, 25:4, 4:1, and 25:16 were examined. Cases 1 to 10 of the finite element analysis by Wang et al. [18] were used to validate the proposed method. Harada et al. [7] exposed ordinary non-tempered glass panels (E = 73 GPa, ρ = 2500 kg/m^3, and α_g = 8.75 × 10^{-6} 1/°C) to heat fluxes ranging between 2.7 kW/m^2 and 9.7 kW/m^2. The size of the glass panels was 500 mm by 500 mm by 3 mm and they were protected at the edges by a frame width of 15 mm. Wang et al. [33] developed a finite element program to investigate the thermal stress distribution during fire exposure. The program was validated using the experiments by Skelly et al. [34] on ordinary non-tempered glass panel (E = 70 GPa and α_g = 9.5 × 10^{-6} 1/°C) exposed

to pool fire. The analyzed glass panels by Wang et al. [33] had a size of 500 mm by 280 mm by 2.4 mm and the width of the supporting frame was 25 mm. Chen et al. [11] exposed ordinary non-tempered glass panels (E = 67.2 GPa, ρ = 2500 kg/m^3, and α_g = 8.46 × 10^{-6} 1/°C) to radiant heating in an enclosed compartment. The glass panel size by Chen et al. [11] was 600 mm by 600 mm by 6 mm and the width of the frame was 30 mm. The measured temperature field was implemented into a finite element program to predict the resultant stresses. Dembele et al. [16] developed a program (Glaz3D) that was validated with ANSYS [35] to study the thermal and mechanical behavior of glazing elements during fire. The validation results are summarized in Fig. 10. As shown in the figure, the proposed approach predicted the fracture tensile strength with an accuracy of ±10%.

Table 1. Validation Cases

Parameter	Wang et al. [18]	Harada et al. [7]	Wang et al. [33]	Chen et al. [11]	Dembele et al. [16]
E, (10^{10} Pa)	6.7	7.3	7.0	6.72	7.3
α_g, (10^{-6} K^{-1})	8.5	8.75	8.5	8.46	8.75
Glass panel size, (m^2)	0.1 to 1 × 0.1 to 1	0.5 × 0.5	0.50 × 0.28	0.6 × 0.6	0.3 × 0.3
Thickness, L (m)	0.006	0.003	0.0024	0.006	0.003
Covered part, b, (m)	0.02	0.015	0.025	0.03	0.015
Max. temperature difference (ºC)	67 – 150	17 – 70	143	133	80

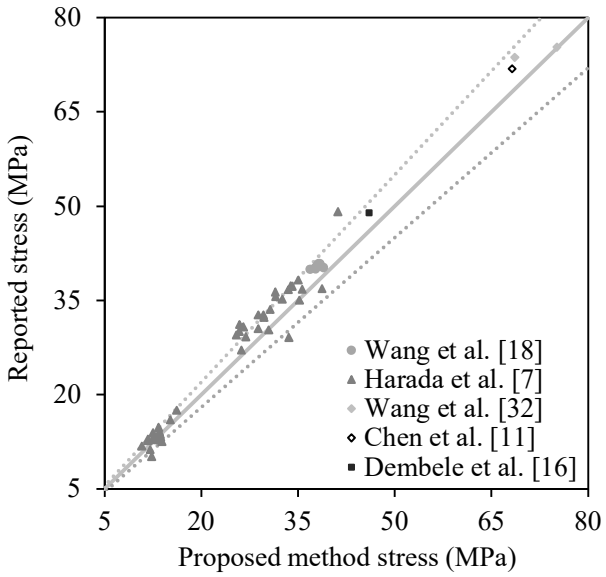

Fig. 10. Validation results

5. Conclusions

This paper provides a simple yet reliable approach to assess the behavior of ordinary glass panels during fire exposure. A set of simplified methods were developed to conduct both heat transfer and stress calculations.

For heat transfer calculations, a simplified method to estimate the temperature at the center of the glass panel was proposed. The method assumes that the temperature across the glass thickness is constant. The finite element method was then utilized to develop an equation that relates the temperature at the edge of the panel to the temperature at its center. The proposed equation suggests that the temperature difference between the glass center and edge increases with the increase of glass thickness and decreases with the increase of the frame width. For stress calculations, a simplified method to estimate the self-induced thermal strains, which maintain the plane section assumption, is developed considering cases of uniform fire exposure and non-uniform fire exposure. Predictions of the proposed approach were compared to the experimental and numerical work by others. The results from the proposed approach confirm

the findings of previous experiments that the self-induced tensile stress increases with the increase of the glass panel dimensions and decreases with the increase of the frame width.

The proposed approach can be utilized to estimate the maximum temperature difference within a glass panel and calculate the developed thermal stresses in glass panels during fire exposure. Future research is needed to extend the applicability of the proposed approach to: (1) other glass types, (2) other conditions of fire exposure, where the resulting temperature of the exposed part of the glass panel is not uniform (partially exposed panel), (3) cases where the heat exchange between the glass and the frame need to be considered, (4) cases with moving air and fire, and (5) glass panels with large dimensions. Notwithstanding these limitations, the comparisons with existing experimental work have confirmed the accuracy of the proposed approach in estimating the maximum tensile stress developed during fire exposure, and thus its accuracy to predict the breakage of ordinary glass, which almost coincides with its cracking [3,7,11,34].

Acknowledgments

The present study was financially supported by the India-Canada Center for Innovative Multidisciplinary Partnerships to Accelerate Community Transformation and Sustainability (IC-IMPACTS), Canada.

References

[1] H.W. Emmons, The needed fire science, in: Fire Saf. Sci. First Int. Symp., IAFSS, 1986: pp. 33–53.

[2] K. Nguyen, P. Weerasinghe, P. Mendis, T. Ngo, J. Barnett, Performance of modern building facades in fire: a comprehensive review, Electron. J. Struct. Eng. 16 (2016) 69–86.

[3] O. Keski-rahkonen, Breaking of Window Glass Close, Fire Technol. 12 (1988) 61–69.

[4] P.J. Pagni, A.A. Joshi, Glass Breaking In Fires, Fire Saf. Sci. 3 (1991) 791–802. https://doi.org/10.3801/IAFSS.FSS.3-791.

[5] C. Bedon, Structural Glass Systems under Fire: Overview of Design Issues, Experimental Research, and Developments, Adv. Civ. Eng. 2017 (2017). https://doi.org/10.1155/2017/2120570.

[6] A.A. Joshi, P.J. Pagni, Fire-induced thermal fields in window glass. II—Experiments, Fire Saf. J. 22 (1994) 45–65. https://doi.org/10.1016/0379-7112(94)90051-5.

[7] K. Harada, A. Enomoto, K. Uede, T. Wakamatsu, An experimental study on glass cracking and fallout by radiant heat exposure, Fire Saf. Sci. (2000) 1063–1074. https://doi.org/10.3801/IAFSS.FSS.6-1063.

[8] T.J. Shields, G.W.H. Silcock, M.F. Flood, Performance of a single glazing assembly exposed to enclosure corner fires of increasing severity, Fire Mater. 25 (2001) 123–152. https://doi.org/10.1002/fam.764.

[9] T.J. Shields, G.W.H. Silcock, M.F. Flood, Performance of a single glazing assembly exposed to a fire in the centre of an enclosure, Fire Mater. 26 (2002) 51–75. https://doi.org/10.1002/fam.783.

[10] P.J. Pagni, Thermal glass breakage, Fire Saf. Sci. (2003) 3–22. https://doi.org/10.3801/IAFSS.FSS.7-3.

[11] H. Chen, Q. Wang, Y. Wang, H. Zhao, J. Sun, L. He, Experimental and Numerical Study of Window Glass Breakage with Varying Shaded Widths under Thermal Loading, Fire Technol. 53 (2017) 43–64. https://doi.org/10.1007/s10694-016-0596-0.

[12] Y. Yang, C.L. Chow, Transient temperature fields and thermal stress fields in glazing of different thicknesses exposed to heat radiation, Constr. Build. Mater. 193 (2018) 589–603. https://doi.org/10.1016/j.conbuildmat.2018.10.106.

[13] Y. Wang, Q. Wang, G. Shao, H. Chen, Y. Su, J. Sun, L. He, J.X. Wen, R. Zong, K.M. Liew, Experimental study on thermal breakage of four-point fixed glass façade, Fire Saf. Sci. 11 (2014) 666–676. https://doi.org/10.3801/IAFSS.FSS.11-666.

[14] A. Vedrtnam, C. Bedon, M.A. Youssef, M. Wamiq, A. Sabsabi, S. Chaturvedi, Experimental and numerical structural assessment of transparent and tinted glass during fire exposure, Constr. Build. Mater. 250 (2020). https://doi.org/10.1016/j.conbuildmat.2020.118918.

[15] Q. Xie, H. Zhang, D. Si, Experimental study on critical breakage stress of float glass with different thicknesses under conditions with temperatures of 25 and 200 C, Fire Mater. 35 (2011) 275–283.

[16] S. Dembele, R.A.F. Rosario, J.X. Wen, Thermal breakage of window glass in room fires conditions - Analysis of some important parameters, Build. Environ. 54 (2012) 61–70. https://doi.org/10.1016/j.buildenv.2012.01.009.

[17] C. Bedon, C. Louter, Thermo-mechanical Numerical Modelling of Structural Glass under Fire - Preliminary Considerations and Comparisons, (2018). https://doi.org/10.7480/cgc.6.2173.

[18] Y. Wang, Y. Zhang, Q. Wang, Y. Yang, J. Sun, The effect of glass panel dimension on the fire response of glass façades, Constr. Build. Mater. 181 (2018) 588–597. https://doi.org/10.1016/j.conbuildmat.2018.06.088.

[19] Y. Yang, L. Miao, C.L. Chow, Relative significance of temperature gradient components on cracking behavior in glass panes under thermal radiation, Appl. Therm. Eng. 131 (2018) 837–848. https://doi.org/10.1016/j.applthermaleng.2017.12.060.

[20] Y. Wang, Q. Wang, Y. Su, J. Sun, L. He, K.M. Liew, Fracture behavior of framing coated glass curtain walls under fire conditions, Fire Saf. J. 75 (2015) 45–58. https://doi.org/10.1016/j.firesaf.2015.05.002.

[21] W. Lu, Y. Wang, H. Chen, L. Jiang, Q. Duan, M. Li, Q. Wang, J. Sun, Investigation of the thermal response and breakage mechanism of point-supported glass facade under wind load, Constr. Build. Mater. 186 (2018) 635–643. https://doi.org/10.1016/j.conbuildmat.2018.07.114.

[22] Y. Wang, J. Hu, Performance of laminated glazing under fire conditions, Compos. Struct. 223 (2019). https://doi.org/10.1016/j.compstruct.2019.110903.

[23] H. Chen, H. Zhao, Y. Wang, Q. Wang, J. Sun, The Breakage of Float Glass with Four-Edge Shading Under the Combined Effect of Wind Loading and Thermal Loading, Fire Technol. 53 (2017) 1233–1248. https://doi.org/10.1007/s10694-016-0630-2.

[24] M. Kozlowski, C. Bedon, D. Honfi, Numerical analysis and 1D/2D sensitivity study for monolithic and laminated structural glass elements under thermal exposure, Materials (Basel). 11 (2018). https://doi.org/10.3390/ma11081447.

[25] F.P. Incropera, D.P. Dewitt, T.L. Bergman, D.S. Lavine, Fundanmentals of Heat and Mass Hransfer, 6th ed., John Wiley, Hoboken, NJ, 1993.

[26] J.P. Holman, Heat transfer, 10th ed., McGraw Hill Higher Education, Boston, 2010.

[27] D. Drysdale, An introduction to fire dynamics, 3rd ed., John Wiley & Sons, Hoboken, N.J, 2011.

[28] Dassault Systemes Simulia, Abaqus 6.14 documentation, Provid. Rhode Island, US. (2017).

[29] International Organization for Standards, ISO 834 - Fire Resistance Tests – Elements of Building Construction, Geneva, Switzerland, 2014.

[30] H. Zhao, Q. Wang, Y. Su, Y. Wang, G. Shao, H. Chen, J. Sun, Experimental Investigation on Glass Cracking for Wind Load Combined with Radiant Heating, in: Fire Sci. Technol. 2015, Springer, 2017: pp. 255–260.

[31] S.F. El-Fitiany, M.A. Youssef, Assessing the flexural and axial behaviour of reinforced concrete members at elevated temperatures using sectional analysis, Fire Saf. J. 44 (2009) 691–703. https://doi.org/10.1016/j.firesaf.2009.01.005.

[32] A.A. Joshi, P.J. Pagni, Fire-Induced Thermal Fields in Window Glass . I—Theory, 22 (1994) 25–43.

[33] Q. Wang, Y. Zhang, Y. Wang, J. Sun, L. He, Dynamic three-dimensional stress prediction of window glass under thermal loading, Int. J. Therm. Sci. 59 (2012) 152–160. https://doi.org/10.1016/j.ijthermalsci.2012.03.018.

[34] M.J. Skelly, R.J. Roby, C.L. Beyler, Experimental investigation of glass breakage in compartment fires, J. Fire Prot. Eng. 3 (1991) 25–34. https://doi.org/10.1177/104239159100300103.

[35] ANSYSInc., ANSYS CFX-Solver, release 10.0, (2005).